We are IntechOpen, the world's leading publisher of Open Access books Built by scientists, for scientists

6,900
Open access books available

186,000
International authors and editors

200M
Downloads

Our authors are among the

154
Countries delivered to

TOP 1%
most cited scientists

12.2%
Contributors from top 500 universities

WEB OF SCIENCE™

Selection of our books indexed in the Book Citation Index
in Web of Science™ Core Collection (BKCI)

Interested in publishing with us?
Contact book.department@intechopen.com

Coordination States and Catalytic Performance of Ti in Titanium Silicalite-1

Yi Zuo, Min Liu and Xinwen Guo

Abstract

In the past two decades, we studied the synthesis, modification, and application of titanium silicalite-1 (TS-1) systematically with the goal of exploring its role as a catalyst for industrial selective oxidation reactions. Three factors were primarily considered for catalytic performance: the coordination states of titanium ions, locations of titanium ions, and diffusion properties. The coordination state of Ti, which was the most important of all the three factors, was tuned by controlling the synthesis conditions and posttreating with organic bases. Spectroscopy was used to help establishing the relationship between catalytic activity and coordination state. More active titanium species were located on the external surface by posttreatment, so the catalytic performance for larger molecules was improved significantly. The diffusion properties can be enhanced by posttreatment with organic bases. Furthermore, meso−/microporous titanium silicalite was synthesized by one-pot synthesis with cetyltrimethyl ammonium bromide (CTAB) as a mesoporous porogen. The TS-1 plate with a short b-axis length was also provided.

Keywords: coordination state, titanium, stability, titanium silicalite-1, selective oxidation

1. Introduction

Natural zeolites are a kind of hydrated crystalline silica-aluminate with specific pore structure. The pore diameters of zeolites are similar to the sizes of molecules. Because they can sieve molecules, they are also known as molecular sieves. According to the pore diameter, IUPAC classified porous materials into microporous materials (<2 nm), mesoporous materials (2–50 nm), and macroporous materials (>50 nm) [1]. Zeolites are a microporous material. Due to their high hydrothermal stability, simple synthesis process, strong adsorption properties, adjustable acidity and alkalinity, and pore shape selectivity, they are widely used in petroleum refining, the chemical industry, and separations [2]. The most commonly used zeolites, such as type-A, faujasite, mordenite, and ZSM-5, have narrow pore size and more serious diffusion restrictions, which are disadvantageous. Mesoporous materials have larger surface areas and pore volumes, which is more favorable for larger molecular reactions, adsorption, and separation. However, the hydrothermal stability is not satisfactory due to the amorphous silica wall of mesopores.

Titanium silicalite-1 (TS-1) with MFI topology was first hydrothermally synthesized by Taramasso et al. [3]. After that, it has attracted much attention due to its excellent catalytic activity for selective oxidation with H_2O_2, such as alkene epoxidation [4–9], aromatics hydroxylation [10–12], ketone ammoximation [13–15], alkane oxidation [16, 17], and so on [18, 19]. Therefore, it is considered a milestone in the field of zeolitic catalysis. MFI topology contains two types of 10-membered ring channels, which are the straight channel (0.56 × 0.54 nm) and zigzag channel (0.55 × 0.51 nm). The substitution of titanium atoms for framework silicon or aluminum atoms generates a molecular sieve with tetrahedrally coordinated Ti. The isolated tetrahedrally coordinated titanium (also called framework Ti) in TS-1 is the main active center for catalytic oxidation. However, the amount of tetrahedrally coordinated Ti is limited (2.5 mol%), because the lattice expansion inhibits the insertion of Ti into the framework [20]. In the next 30 years, phenol hydroxylation to benzene diols, cyclohexanone ammoximation to cyclohexanone oxime, butanone ammoximation to diacetyl monoxime, and propene epoxidation to propene oxide catalyzed by TS-1 were commercialized successively. Nevertheless, there are still many problems in the synthesis and application of TS-1, such as the transformation of tetrahedrally coordinated Ti to octahedrally coordinated Ti or anatase TiO_2 (loss of the active center) in the reaction, and the deactivation of the catalyst by blocking of channels [21]. Therefore, many researchers have made an effort to solve these problems, and so do we. To further improve the catalytic performance and expand the application of TS-1, it is necessary to summarize our current research achievement.

In this chapter, we describe our recent progress on controlling Ti coordination states, design of porosity, and applications of TS-1. We hope that this summary will help in understanding the developing process and our contribution to research on TS-1.

2. Controlment of the Ti coordination states

2.1 Tuning of synthesis conditions

There are mainly three kinds of Ti species in TS-1. Tetrahedrally coordinated titanium, which was mentioned above, is usually considered to be the active center for the oxidation reactions. This Ti species can form a five-membered ring (5MR) structure with hydrogen peroxide and alcohol (see **Figure 1**) [22], which can oxidize propene to prepare propene oxide. The 5MR structure is very stable and is easy to be formed in the epoxidation of alkenes, according to density functional theory study. The β-O atom in the structure is partially positive due to the hydrogen bond between alcohol and O-O-H; thus, the C=C bond can react with the β-O atom by nucleophilic attack. The 5MR mechanism explains the effects of alcohol solvents
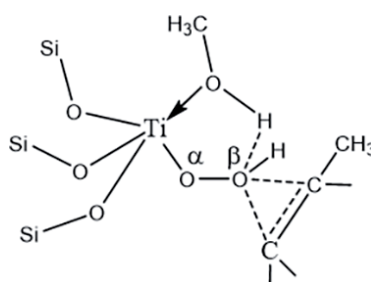
Figure 1.
Diagram of 5MR structure.

in propene epoxidation well; hence it is widely accepted. The other two types of Ti species in TS-1 are octahedrally coordinated Ti (usually called extra-framework Ti) and anatase TiO_2. When the feeding amount of titanium source in the synthesis gel is more than 2.5 mol%, the excessive Ti will transform to these two Ti species. The anatase TiO_2 can decompose hydrogen peroxide to water and O_2; thus, the generation of anatase TiO_2 should be avoided [23]. The octahedrally coordinated Ti can be generated from the tetrahedrally coordinated Ti coordinating with two water molecules. The function of octahedrally coordinated Ti is still controversial. Former researchers thought it was inert for oxidation, but recent works have reported that it was also active for selective oxidation [24]. Wang et al. found that octahedrally coordinated Ti is an intermediate in propene epoxidation [25].

It is well known that the hydrolysis rate of titanium sources is faster than that of silicon sources and the similar hydrolysis extent or crystallization rates of them benefit for the generation of more tetrahedrally coordinated Ti. Therefore, we hydrolyzed the two sources individually to complete hydrolysis simultaneously [26]. Tetrapropylammonium hydroxide (TPAOH) was used as template and base and was added to silicon and titanium sources. The silicon source was hydrolyzed at 313 K for 5 h, while the titanium source was at room temperature for 0.5 h. The hydrolysis of the two sources was completed at the same time. After that, the two hydrolysates were mixed together and crystallized at 443 K for 2 d. Under these conditions, the content of tetrahedrally coordinated Ti in TS-1 was ~1 wt%, while the total content of Ti was ~1.9 wt%. From this result, we know that the generation of tetrahedrally coordinated Ti is difficult.

Until now, tetrapropylammonium ions (TPA$^+$) are necessary for synthesizing TS-1 as the template. In consideration of the high price of TPAOH, many researchers tend to use tetrapropylammonium bromide (TPABr) to structure-directly synthesize TS-1 because they have the same TPA$^+$ cation, but TPABr is much cheaper. However, due to the introduction of Br$^-$ and the reduction of basicity, the particle size of TS-1 enlarges obviously when TPABr is used. The TPAOH system often obtains nanosized TS-1, while the TPABr system usually gets microsized particles. We explored a method for synthesizing small-crystal TS-1 in the TPABr system [27], which will be presented in detail in Section 3.1. Herein, we only discuss the influence of molar ratio of Si/Ti (n(Si/Ti)) on the coordination states of Ti when synthesizing small-crystal TS-1 in the TPABr system. Small-crystal TS-1 with different feeding n(Si/Ti) (20, 50, and 80) was synthesized by adding different amounts of titanium source (TiCl$_4$) to the synthesis gel. The weight content of silicon and titanium in the samples obtained by inductively coupled plasma-optical emission spectrometer (ICP-OES) shows that the actual n(Si/Ti) was slightly higher than the feeding one, except for sample with the feeding n(Si/Ti) of 20. Ultraviolet/visible diffuse reflectance (UV/vis) spectroscopy, Raman spectroscopy, and X-ray adsorption near edge structure (XANES) spectroscopy were used to study the coordination states of Ti qualitatively and quantitatively [28].

UV/vis spectroscopy is one of the first spectral techniques used for the detection of Ti coordination states in titanium silicalites. Peak deconvolutions were performed using the PeakFit program with the Gaussian fitting method. In the spectra of small-crystal TS-1 (**Figure 2**), there are three major absorption bands centered at 200–210, 230–290, and 310–330 nm. The band at 200–210 nm is assigned to tetrahedrally coordinated Ti, while that at 310–330 nm belongs to anatase TiO_2. There are more than one kind of Ti species between 230 and 290 nm in the UV/vis spectra of TS-1. The band at approximately 250–290 nm is attributed to the octahedrally coordinated Ti species, which is inactive for the oxidation reactions, and the band at 230–250 nm is an isolated Ti species with a lower coordination number of oxygen than octahedrally coordinated Ti (such as pentahedrally coordinated Ti). The

undercoordinated Ti has a higher energy than the octahedral one, so its band shifts to a shorter wavelength. The content of tetrahedrally coordinated Ti, octahedrally coordinated Ti, and anatase TiO_2 increases when $n(Si/Ti)$ is decreased, and the increase of anatase TiO_2 content is much stronger than that of other species, proving that the introduction of Ti in the framework is limited. It is notable that a new band appears at ~235 nm in the sample with $n(Si/Ti)$ of 80. We consider it to belong to the pentahedrally coordinated Ti by combining these results with the results of XANES. This Ti state might be formed by one Ti atom with five "SiO_4". Thus, a high $n(Si/Ti)$ promotes more "SiO_4" coordination with this Ti atom, which is beneficial to the generation of pentahedrally coordinated Ti.

The catalytic performance of the small-crystal TS-1 with different $n(Si/Ti)$ was evaluated in the epoxidation of propene. The conversion of H_2O_2 over TS-1 with $n(Si/Ti)$ of 20 is the lowest, indicating that the Ti coordination state is more important than its content for the catalytic activity. The highest turnover frequency (TOF) was obtained from the TS-1 with $n(Si/Ti)$ of 80, demonstrating that the pentahedrally coordinated Ti was the most active species of all the Ti coordination types. The lowest TOF was obtained over the TS-1 with $n(Si/Ti)$ of 20, indicating that octahedrally coordinated Ti was inert or had negative effects on the epoxidation. Based on the XANES and TOF data, we calculated the contents of differently coordinated Ti in the three samples (see **Table 1**). The content of pentahedrally coordinated Ti decreases and the content of octahedrally coordinated Ti increases with the decrease of feeding $n(Si/Ti)$ from 80 to 50, suggesting that the insertion of Ti into the framework is at nearly the maximum at the $n(Si/Ti)$ of 80. Continuing to add Ti leads to a sharp increase of octahedrally coordinated Ti. The TOFs of pure tetrahedrally, pentahedrally, and octahedrally coordinated Ti in small-crystal TS-1, which were calculated according to the total TOFs and contents of differently coordinated Ti, are 373.3, 1434.3, and 0 mol H_2O_2/(h·mol Ti), respectively. These results confirm that pentahedrally coordinated Ti is the most active species among the three coordination structures.
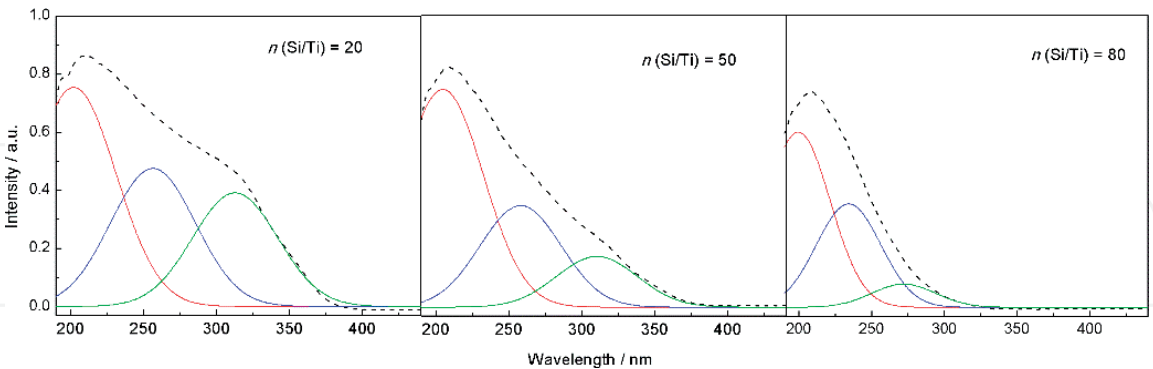
Figure 2.
UV/Vis spectra of the TS-1 with different n*(Si/Ti).*

$n(Si/Ti)$	Percentage of differently coordinated Ti/%		
	Tetrahedral Ti	Pentahedral Ti	Octahedral Ti
20	42	0	58
50	76	21	3
80	50	50	0

Table 1.
*Contents of differently coordinated Ti.*

Nevertheless, the controllable synthesis of TS-1 with a large amount of pentahedrally coordinated Ti is still impossible. When more Ti was added to the synthesis gel, the pentahedrally coordinated Ti would transform to tetrahedrally and octahedrally coordinated Ti due to the loss of pentahedrally coordinated Ti generation conditions mentioned previously.

In addition, the stability sequence of differently coordinated Ti is anatase TiO_2 > octahedrally coordinated Ti > tetrahedrally coordinated Ti > pentahedrally coordinated Ti. The catalytic activity sequence is opposite to the stability, because unstabilization means high energy and thus high catalytic activity.

2.2 Usage of additives

From the above introduction, we know that matching the crystallization rates of silicon and titanium sources benefits the generation of tetrahedrally coordinated Ti. Therefore, some researchers tried to control the crystallization process by adding some modifiers. Fan et al. used different ammonium salts as the crystallization-mediating agents to synthesize TS-1 [29]. They found that the ammonium salts could not only drastically decrease the pH of the synthesis gel and slow down crystallization, but they could also modify the crystallization mechanism and make the incorporation of titanium into the framework match well with that of silicon. As a result, the formation of octahedrally coordinated Ti and anatase TiO_2 was eliminated successfully. It was reported that the anionic polyelectrolyte poly(acrylic acid) was also able to facilitate the insertion of Ti to the framework via a liquid-phase and solid-phase transformation mechanism [30]. Some researchers used sucrose as the modifier [31], which would carbonize during the crystallization of TS-1 and release hydrogen ions. Therefore, the pH of the hydrothermal system was reduced, and the sucrose played a similar role to the ammonium salts.

We adopted two natural macromolecular additives to adjust the coordination states of Ti, which were starch and gelatin [32]. When they were introduced to the synthesis gel, they also released hydrogen ions as the sucrose did. Hence, they can also tune the coordination states of Ti.
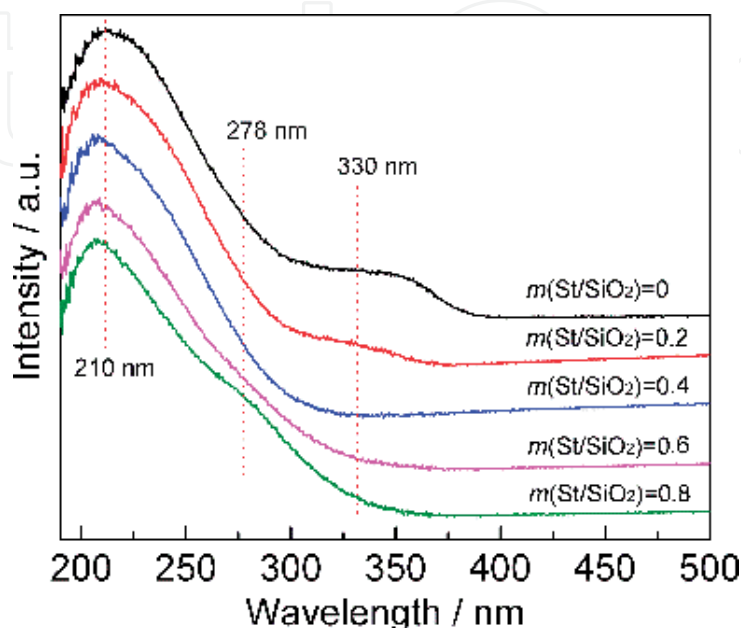
Figure 3.
UV/Vis spectra of the TS-1 synthesized with different amounts of starch.

The addition of starch hardly influences the morphology of TS-1 but can eliminate the formation of extra-framework Ti. **Figure 3** shows the UV/vis spectra of TS-1 synthesized with different amounts of starch. An obvious absorption band at ~330 nm appears in the TS-1 synthesized without starch, proving the existence of anatase TiO_2. As the content of starch and gelatin increases, the band of anatase TiO_2 disappears gradually. The content of octahedrally coordinated Ti decreases with the increase of starch until the weight ratio of starch/SiO_2 (m(St/SiO_2)) reaches 0.6. Then, the content of octahedrally coordinated Ti increases slightly, probably due to the introduction of starch promoting the coordination saturation of titanium ions. Compared to the TS-1 synthesized without starch, those obtained with starch have a higher content of tetrahedrally coordinated Ti, a quite low content of octahedrally coordinated Ti, and are free of anatase TiO_2. Therefore, they show a much higher catalytic activity for the epoxidation of 1-butene.

Gelatin is similar to starch in its effect on Ti coordination states. However, it contains both amino and carboxyl groups. Thus, it has the ability to tune the morphology of MFI-typed zeolites. This will be further discussed in Section 3.4.

### 2.3 Posttreatment with organic bases

Many studies focused on the treatment of zeolites with organic bases, especially for the quaternary ammonium bases, because the treatment could improve the catalytic performance significantly. The treatment leads to the dissolution of "SiO_4" in the TS-1 crystals and recrystallization on the external surface of crystals, generating hollow zeolites, which decreases the diffusion resistance. When the "SiO_4" was dissolved, the coordination states of the neighbored Ti ions would be changed accordingly. Two Si-O bonds near to the tetrahedrally coordinated Ti may be broken, and the tetrahedrally coordinated Ti may transform to octahedrally coordinated Ti after combining with two water molecules (**Figure 4**).

We studied the treatment of small-crystal TS-1 with different organic bases, including ethylamine (EA), diethylamine (DEA), tetramethylammonium hydroxide (TMAOH), and tetrapropylammonium hydroxide (TPAOH) solutions [33]. The catalytic performances of phenol hydroxylation over the treated samples were improved to different extents. The TS-1 treated with TPAOH has the highest catalytic activity in the treated samples.

To understand the reason for this result, we characterized the treated samples with Ti L-edge XANES spectroscopy, the spectra of which are shown in **Figure 5**. The spectra consist of two sets of doublets, which correspond to the $2p_{1/2}$ and $2p_{3/2}$ transitions of the $3d^0$ to $2p^5 3d^1$ states. The $L2$ edge is at a higher energy (462–470 eV), and the $L3$ edge is at a lower energy (455–462 eV). The splitting of each edge is attributed to the t_{eg} and e_g symmetry of the d orbital.
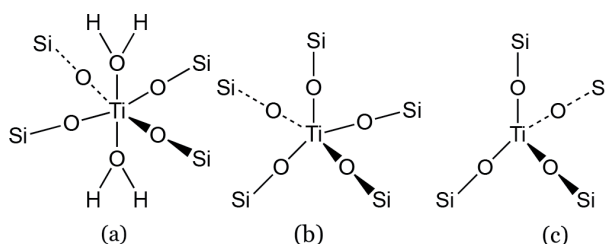
Figure 4.
Structures of octahedrally coordinated Ti (a), pentahedrally coordinated Ti (b), and tetrahedrally coordinated Ti (c).
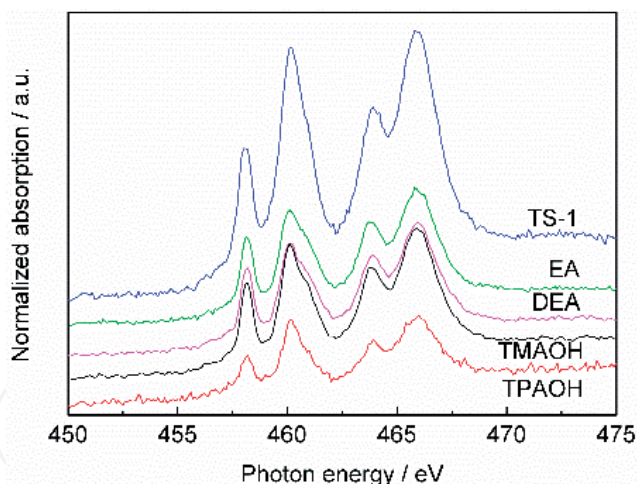
Figure 5.
Ti L-edge XANES spectra of the TS-1 treated with different bases.

The higher energy peak of the $L3$ edge (459–462 eV) consists of two peaks in some samples, a main peak and a shoulder one, which is on the lower energy side (~460 eV) for rutile TiO_2 and the higher energy side (461 eV) for anatase TiO_2. The intensities of the two peaks are reversed for the substances that they represent. The tetrahedrally coordinated Ti is characterized by the absence of splitting of the peak at 459–462 eV and a relatively weaker intensity of the peaks at lower energies of both the $L2$ and $L3$ edges than those at higher energies. The pentahedrally coordinated Ti is characterized by a slight shift to higher energy and a drastic decrease of the lower energy peak of $L3$, a shift of the higher energy peak of $L2$ to lower energy, and the appearance of a shoulder peak on the lower energy peak of $L2$. We found that pentahedrally coordinated Ti existed in the TPAOH-treated TS-1, but it was absent in the other samples. Therefore, the generation of pentahedrally coordinated Ti is another reason for the increasing activity of TPAOH-treated TS-1. The possible structure of pentahedrally coordinated Ti is shown in **Figure 4**, the stable form of which is tetragonal pyramid.

3. Improvement of the diffusion property

3.1 Reducing of particle size in TPABr system

Most reactions catalyzed by zeolites occur in their channels. A short channel means a short diffusion pathway for reactants from bulk to active centers (such as tetrahedrally coordinated Ti), therefore reducing the particle size benefits the diffusion. We have mentioned in Section 2.1 that the particle size of TS-1 obtained in the TPABr hydrothermal system is often at the micron scale, which is disadvantageous for diffusion. Hence, we tried to control the particle size of TS-1 in the TPABr system by adding different seeds. First, we used the mother liquor of nanosized TS-1 as the seed [27]. The synthesis process is illustrated in **Figure 6**. The mother liquor was prepared by crystallizing the synthesis gel at 443 K for 48 h, according to prior work [26]. The size of the obtained seed is ~100 nm. When using powdery TS-1 as the seed, microsized TS-1 was obtained, the size of which was 2 × 1 × 0.5 μm. However, when the seed was changed to the mother liquor, the size decreased significantly to 600 × 400 × 250 nm, so we called it small-crystal TS-1. Its catalytic performance was evaluated in the epoxidation of propene and hydroxylation of phenol. The conversion of H_2O_2 and selectivity of
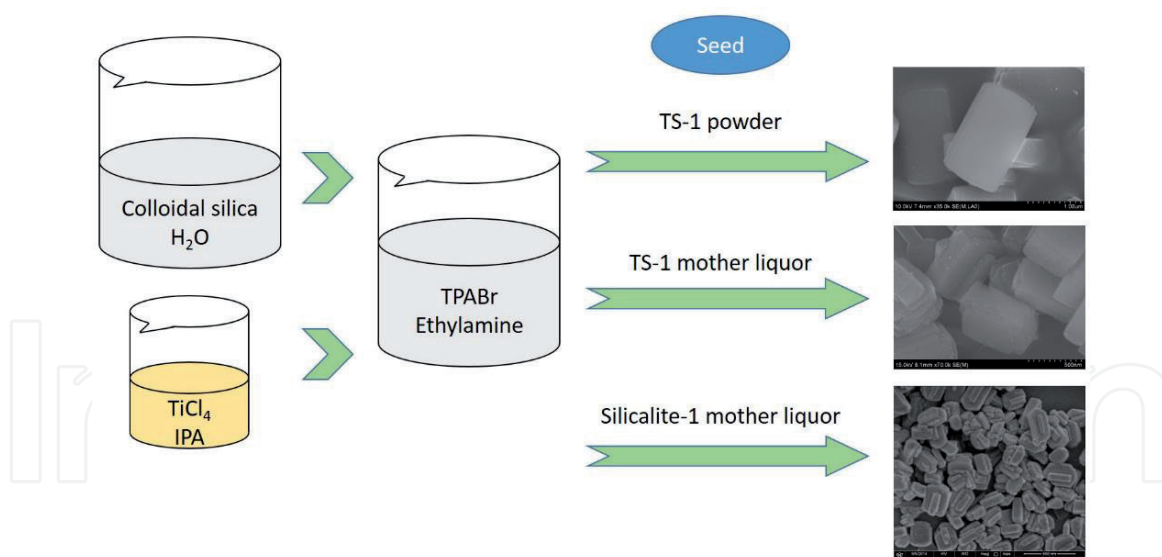
Figure 6.
Synthesis process of TS-1 in TPABr system.

PO on small-crystal TS-1 reached 92 and 98%, respectively. In the hydroxylation of phenol, using small-crystal TS-1 as a catalyst also resulted in a higher conversion of phenol.

The synthesis conditions were then systematically studied, including purification methods for small-crystal TS-1, the Si/Ti molar ratio in TS-1, the amount of the seed, and the crystallization period [34]. It was found that the size of TS-1 was not significantly affected by the synthesis conditions except for the amount of seed. The highest catalytic performance of the propene epoxidation was obtained when the TS-1 was purified three times by precipitation; the n (Si/Ti) was 50, the weight ratio of seed/SiO$_2$ was 0.06, and the crystallization time was 48 h.

After that, the seed was changed to the mother liquor of nanosized silicalite-1, the size of which was ~80 nm [35]. The particle size can be adjusted from 1200 to 200 nm by varying the seed amount from 0.05 to 12 wt%. The relationship between particle size and the content of seed is shown in **Figure 7**. The data fits well to a power function, with the fit equation of:

$$\text{Crystal size} = 468.7 \, (\text{content of seed})^{-0.3158} \tag{1}$$

The degree of fitting measured by the coefficient of determination (R^2) is 0.9968. Crystallization time plays a less important role than seed amount on the adjustment of the size. TS-1 with different crystal sizes was characterized and evaluated in the propene epoxidation. The catalytic activity and selectivity for PO are enhanced by decreasing the particle size from 1200 to 200 nm, due to gradually eliminated diffusion limitations. The seed is significant for this system, because eliminating the seed leads to poor crystallization and catalytic activity. The mechanism of the seed function was studied by simulating the transformation process of the seed in the TS-1 synthesis system. When the content of seed is lower than 1 wt%, it primarily performed as a nucleus for the growth of silicon and titanium sources. As the content increases, more seed will dissolute to secondary structural units first and then accelerate the crystallization.

Furthermore, the low pH of the TPABr system promotes the similarity of crystallization rates of silicon and titanium sources, inhibiting the generation of
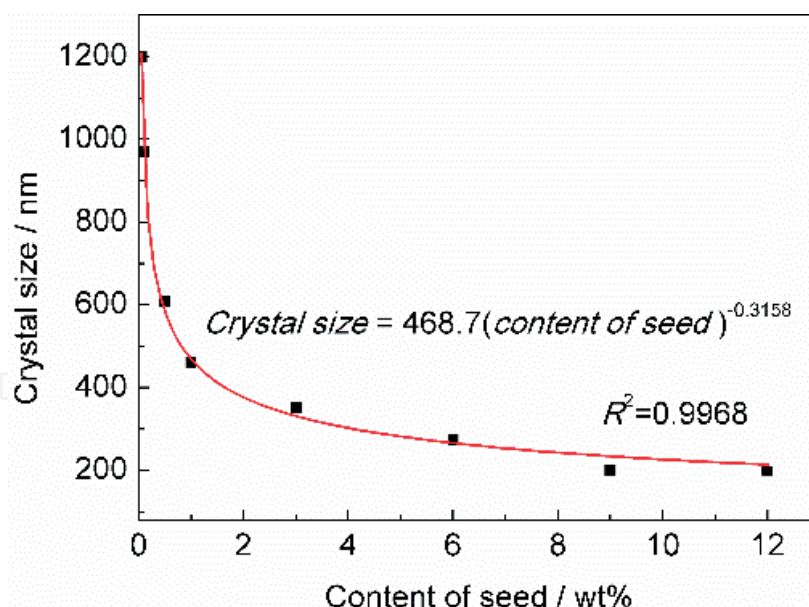
Figure 7.
Particle size of TS-1 plotted against the weight percent of seed using in synthesis. (data points represent experimental data, and the continuous curve represents a power law fit to the data with equation given on the plot).

octahedrally coordinated Ti and anatase TiO_2. The content of tetrahedrally coordinated Ti achieved ~1.2 wt% when the feeding $n(Si/Ti)$ was 50.

3.2 Design of hollow TS-1 materials

In addition to reducing the particle size, synthesis of hollow materials can also enhance diffusion properties. Treating with TPAOH solution is one of the most commonly used methods for generating hollow spaces in TS-1. However, this method leads to the transformation of tetrahedrally coordinated Ti to extra-framework Ti, which is harmful for the catalytic performance. Therefore, we provided a method for synthesizing a hollow core-shell material to prevent the generation of extra-framework Ti [36]. The hollow silicalite-1@titanium silicalite-1 (H-S-1@TS-1) core-shell material was synthesized in a TPAOH hydrothermal system with hollow silicalite-1 serving as the core (see **Figure 8**). The very small TS-1 particles grow along the external surface of hollow silicalite-1, thus generating hollow material. Since the hollow structure was given by silicalite-1, the tetrahedrally coordinated Ti in H-S-1@TS-1 was not converted to other coordination states. Thus, the extra-framework Ti was absent in H-S-1@TS-1. Due to the synergy function of pure tetrahedrally coordinated Ti species, higher Ti content on external surface, and enhanced diffusion properties, H-S-1@TS-1 showed better propene epoxidation activity (TOF = 13.61 mol/(mol·h)) than traditional microporous TS-1 (TOF = 8.08 mol/(mol·h)) and that posttreated with TPAOH solution (TOF = 9.75 mol/(mol·h)).

3.3 Insertion of Ti on the external surface

In the posttreatment with TPAOH solution, the "SiO4" in the crystals is dissolved and recrystallized on the external surface. When TS-1 was extruded with silica as the support and the obtained extrudate was treated with TPAOH solution, the silica support would crystallize and restrain the dissolution of "SiO_4" in the crystals [37]. Hence, we introduced a titanium source to the posttreatment to make it crystallize
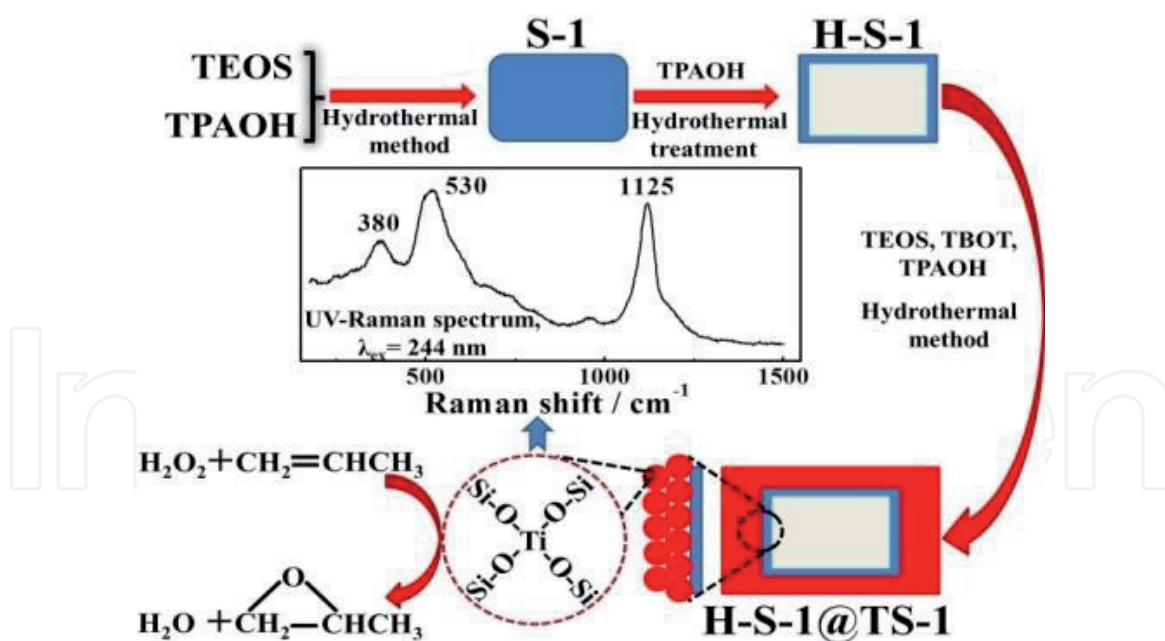
Figure 8.
Preparation process of H-S-1@TS-1.

Ti content/vol%	In the bulk			On the surface		
	SiO$_2$/wt%	TiO$_2$/wt%	n(Si/Ti)	SiO$_2$/wt%	TiO$_2$/wt%	n(Si/Ti)
Untreated	97.06	2.79	46.4	98.67	1.18	111.9
0	97.10	2.76	46.9	98.99	0.86	153.5
5	96.96	2.89	44.8	98.51	1.34	98.1
10	96.81	3.02	42.7	98.29	1.54	85.3
16	96.73	3.12	41.4	98.28	1.57	83.6
25	96.65	3.20	40.3	98.25	1.60	81.7

[a]*The elemental compositions in the bulk and on the surface were determined by ICP-OES and XPS, respectively.*

Table 2.
Elemental composition of the TS-1 treated with different Ti contents[a].

with silica support and insert more Ti on the external surface [38]. Different amounts of the titanium source (tetrabutyl titanate hydrolysate) were added to the TPAOH solution. **Table 2** shows the elemental compositions of the samples both in the bulk and on the external surface. The n(Si/Ti) in the bulk is hardly affected by the individual TPAOH treatment. The Ti content increases gradually with increasing concentration of Ti in the postsynthesis solution. However, not all Ti in the samples transforms to tetrahedrally coordinated Ti. The X-ray photoelectron spectroscopy (XPS) results show that the content of Ti on the external surface reduced after the treatment with TPAOH solution, which is probably due to the crystallization of amorphous silica occurring at the external surface of TS-1 particles and covering more Ti species. The n(Si/Ti) on the external surface decreases as Ti concentration in the postsynthesis solution increases, indicating that Ti can be located at the external surface under these postsynthesis conditions, and the amount of Ti is restricted by the Ti concentration and the limitation of Ti in the MFI topology. The samples were evaluated in the hydroxylation of phenol. The conversion of phenol increases to a different extent after the postsynthesis. The hollow spaces generated in the crystals

reducing the diffusion limitation may be one of the reasons for the improvement of catalytic activity. The new generated tetrahedrally coordinated Ti on the external surface also provides more easily adsorbable active centers for reactants. At low Ti concentrations ($\leq$10 vol%), increasing the Ti amount generates more active Ti centers on the external surface. Thus, the conversion of phenol increases as Ti concentration increases. However, at high Ti concentrations, the excessive Ti is converted to anatase TiO_2 due to the limitation of titanium content in the MFI topology. The anatase TiO_2 can block the channels and cover the active centers. Thus, the conversion decreases as Ti concentration increases over 10 vol%.

3.4 Preparation of plate-like TS-1

We have mentioned in Section 2.2 that adding gelatin to the synthesis gel of TS-1 could modify its morphology. Actually, it can adjust the thickness of the *b*-axis of MFI-type zeolites. The *b*-axis direction is parallel to the straight channel, so the short, straight, and open channels of zeolites with MFI topology are tailored for diffusion and catalysis. Ti-MFI, Al-MFI, Zr-MFI, Mn-MFI, Cu-MFI, and Fe-MFI plates were synthesized with *b*-axis lengths ranging from 40 to 200 nm by these means. The lengths of the other two dimensions are submicron-sized, which leads to an easy separation of zeolites from the mother liquor. The synergistic effects of the amino and carboxyl groups in gelatin lead to the generation of plate-like zeolites. The physical adsorption of cyclohexane indicates that TS-1 with a thickness of 40 nm has a faster diffusion rate than that of the traditional aggregated material. The TOF of cyclohexene epoxidation over TS-1 plates is about four times that of traditional nanosized TS-1.

3.5 One-pot synthesis of meso−/microporous titanium silicalite

In recent years, research on the synthesis of hierarchical molecular sieves has attracted much attention, because they have the advantages of microporous (good catalytic activity and hydrothermal stability) and mesoporous (excellent diffusion property) materials simultaneously. The preparation methods of hierarchical molecular sieves are mainly postsynthesis and one-pot synthesis. The postsynthesis method uses acid or base to treat micropores, which was introduced above. One-pot synthesis of hierarchical titanium silicalite was first reported by Jacobsen et al. using carbon black as a hard template [39]. After that, a series of hierarchical titanium silicalites were synthesized by using different carbon-based materials. However, the complexity of the synthesis procedure seriously limited the industrial applications of these hierarchical materials. An attractive method is to utilize suitable surfactants as soft mesoporous templates for the direct synthesis of hierarchical materials. Cetyltrimethyl ammonium bromide (CTAB) is one of the most commonly used surfactants. Nevertheless, the mesopores in the CTAB-directed materials are mostly intercrystals. Furthermore, the micropores and mesopores are often phase-separated from each other. We explored an easy and new route for synthesizing the meso−/microporous titanium silicalite with controllable pore diameter by using CTAB and TPAOH as mesoporous and microporous template, respectively [40]. The new route is adding CTAB to the hydrolysis reaction of the silicon source so it forms mesopores prior to the crystallization of microporous MFI topology and prevents the occurrence of phase separation. In other words, this porosity formation sequence makes the two kinds of channels in the materials, which are micropores with MFI topology and mesopores with worm-like morphology, distributed homogeneously. The pore diameter of the mesopores can be adjusted from the maximum
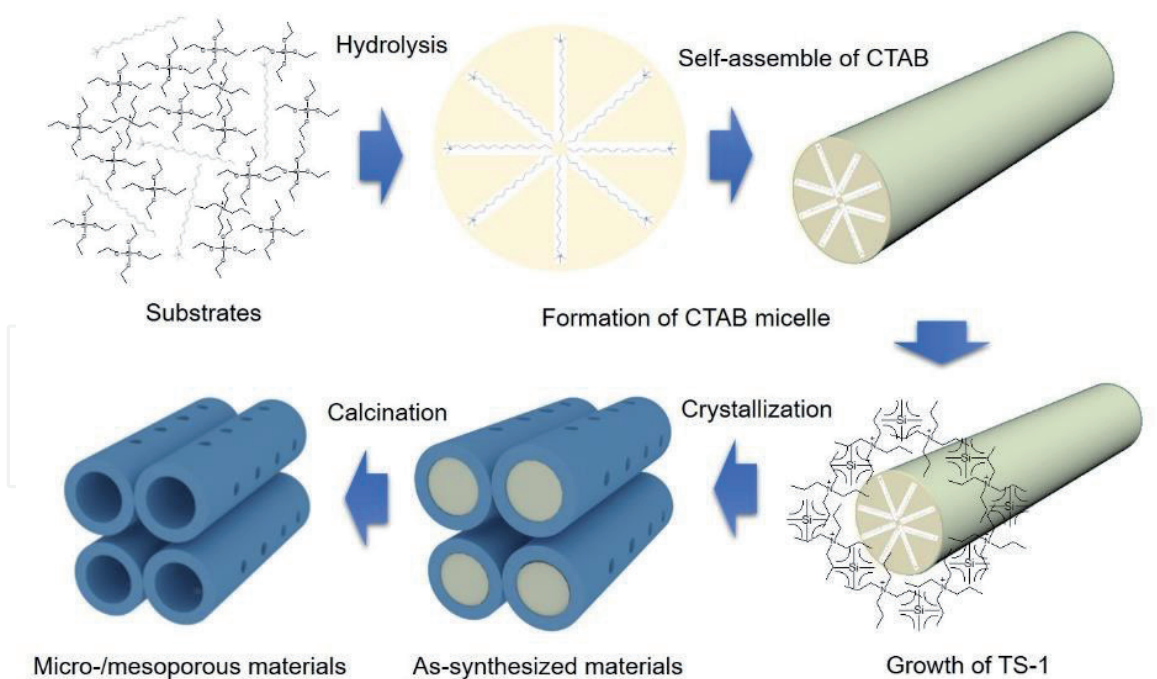
Figure 9.
*Synthesis process of meso−/microporous titanium silicalite.*

center of 2.6 nm to that of 6.9 nm by tuning the molar ratio of CTAB to silicon from 0.125 to 0.20. The introduction of CTAB also causes the variation in coordination states and location of Ti ions in the materials. More CTAB leads to a higher content of octahedrally coordinated Ti and a lower content of tetrahedrally coordinated Ti. Furthermore, more Ti is located near the external surface of TS-1 crystals, when adding more CTAB to the synthesis gel.

The meso−/microporous titanium silicalite catalysts were evaluated in the epoxidation of cyclohexene and showed excellent catalytic activity with respect to the conventional microporous TS-1, due to the enhanced diffusion properties in the mesopores and higher titanium content near the external surface of the former (**Figure 9**).

4. Industrial application of HPPO route

PO is an important organic chemical intermediate among propene derivatives. Most PO is used to produce polyether polyols and polyurethane. Since 2003, the consumption of PO in the world has been increasing year by year. There are about 20 routes for PO production, among which the Chlorohydrin and Halcon routes are the most commonly used. The investment cost of Chlorohydrin route is low, but it produces a large amount of wastewater containing Cl^-, which pollutes the environment and seriously corrodes equipment. The Halcon route overcomes the disadvantages of environmental pollution, but the cost is high. Moreover, the economy of PO is seriously affected by the coproducts. Therefore, PO manufacture needs a new route.

At present, hydrogen peroxide to propene oxide (HPPO) route is one of the most possible alternatives for PO production. Compared to the traditional routes, the HPPO route provides environmental and economic benefits. In recent years, the HPPO route was commercialized by BASF/Dow Chemical and Evonik/Uhde in Belgium and South Korea, separately. Some institutes also tried this route in pilot plants. The main and side reactions in HPPO route are shown in **Figure 10**. It is clear that all the reactions are exothermic. The exothermic reaction not only
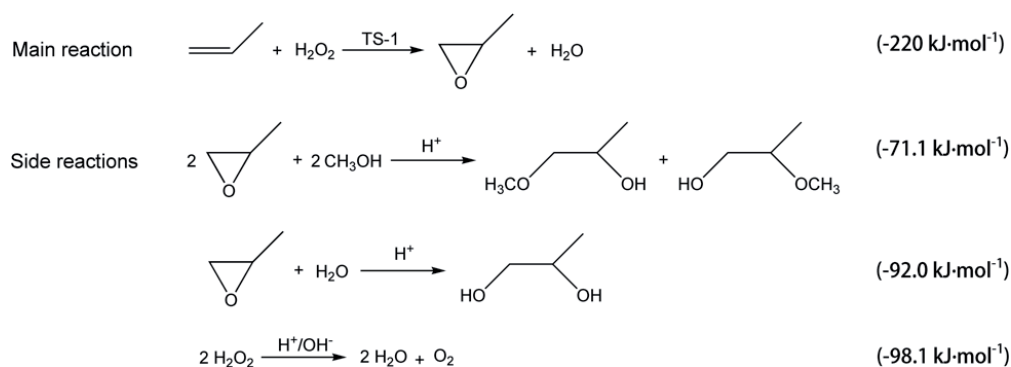
Figure 10.
Main and side reactions in HPPO route.
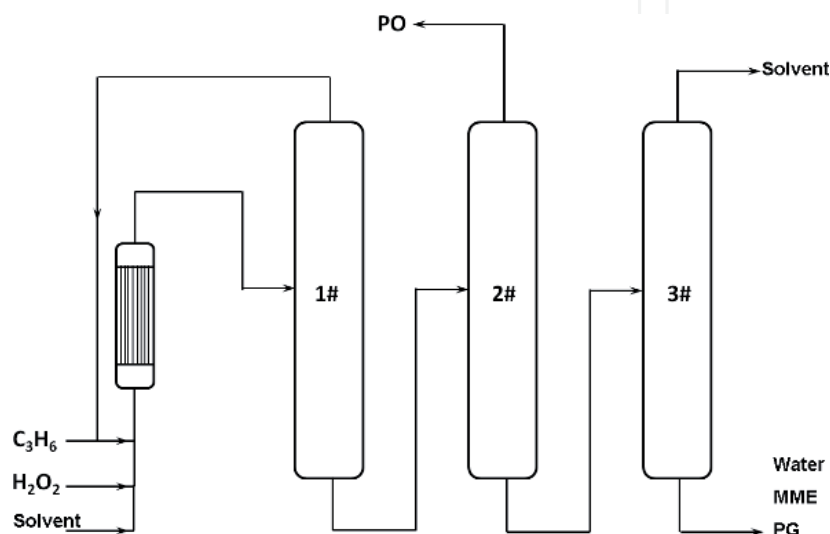
Figure 11.
Flow chart of the 100 t/a HPPO pilot plant.

threatens safety but also promotes the solvolysis reactions and generates PO oligomers. The blocking of TS-1 channels by oligomers is the main cause for its deactivation.

Three steps were taken for the industrialization of our HPPO route, which were the 100 t/a pilot plant, 1000 t/a pilot plant, and 150 kt/a industrial plant. In 2009, the 100 t/a pilot plant procedure was carried out in Jiangsu, China, the flow chart of which is shown in **Figure 11**. A fixed-bed reactor was adopted, and the loading of the catalyst was 100 kg. Propene, H_2O_2, and solvent were fed into the reactor simultaneously by three pumps. The product flowed out of the reactor and entered the 1# rectifying column, in which propene was separated from the top of the column. Then, propene flowed to the propene storage tank for recycling. The materials from the bottom of the 1# rectifying column entered the 2# rectifying column. PO was separated from the top of this column and entered the finished tank. The materials from the bottom of the 2# rectifying column entered the 3# rectifying column. The solvent was separated from the top of the column and put into the solvent storage tank for recycling. The material in the bottom of the column contained mainly water and a small amount of MME and PG.

The 1000 t/a pilot plant and 150 kt/a industrial plants used similar technology to the 100 t/a pilot plant, except for some energy optimization. The former was carried out in 2013, while the latter is under construction. Under the optimized reaction conditions, the conversion of H_2O_2 and selectivity of PO are both higher than 95%, and the purity of PO is more than 99.95% in the three HPPO routes.

The industrial catalyst deactivated partly after the 100 t/a pilot plant reaction. The activity decreased from the inlet to the outlet of the pilot plant reactor [41]. The main reason for the deactivation in pilot plant is similar to that in laboratory, which is blocking of pores and covering of active centers by ethers or oligomers. The more oligomers are generated, the more seriously the catalyst deactivates. The loss of a small amount of framework titanium had little influence on the catalytic activity.

The deactivated catalysts could be externally regenerated by calcination at 813 K for 6 h and in situ regenerated by washing with dilute H_2O_2. The in situ regeneration, rather than the external regeneration, can be adopted in industry. When using in situ regeneration with dilute H_2O_2, a longer washing time is more effective than a higher concentration of H_2O_2. There is one thing needing to be concerned for in situ regeneration. If the concentration of H_2O_2 is too high or the washing time is too long, some tetrahedrally coordinated Ti will be leached out and transform to octahedrally coordinated Ti.

5. Conclusions

Great progress has been made in the synthesis of TS-1 and improvement of its catalytic properties. The relative technologies have become increasingly more mature. However, the active center in TS-1 is still controversial (tetrahedrally, pentahedrally, and/or octahedrally coordinated Ti). The contradiction between the cost and catalytic performance of TS-1 has not been resolved completely. Therefore, the synthesis of high-performing, low cost TS-1 needs to be further studied. At present, people attach great importance to environmental protection; thus, the application of TS-1 will have broad development.

This chapter summarized recent work by our group on TS-1, including the tuning of coordination states of Ti, improvement of diffusion properties, and industrial applications of the HPPO route. We hope to provide some references for related research.

Acknowledgements

Conflict of interest

There is no conflict of interest to be declared.

Author details

Yi Zuo, Min Liu and Xinwen Guo*
State Key Laboratory of Fine Chemicals, PSU-DUT Joint Center for Energy
Research, Department of Catalysis Chemistry and Engineering, School of Chemical
Engineering, Dalian University of Technology, Dalian, China

*Address all correspondence to: guoxw@dlut.edu.cn

IntechOpen

References

[1] Rouquerol J, Avnir D, Fairbridge CW, Everett DH, Haynes JM, Pernicone N, et al. Recommendations for the characterization of porous solids. Pure and Applied Chemistry. 1994;**66**:1739-1758. DOI: 10.1351/pac199466081739

[2] Chen S, Wang Q. Scientific Fundamentals and Technologies for Preparation of Solid Catalysts. Beijing: Chemical Industry Press; 2012. pp. 110-111. DOI: 9787122147165

[3] Taramasso M, Perego G, Notari B. Preparation of porous crystalline synthetic materials comprised of silicon and titanium oxides. US Patent. 1983;4410501

[4] Clerici MG, Bellussi G, Romano U. Synthesis of propylene oxide from propylene and hydrogen peroxide catalyzed by titanium silicalite. Journal of Catalysis. 1991;**129**:159-167. DOI: 10.1016/0021-9517(91)90019-Z

[5] Zhang Z, Kong XX, Feng M, Luo ZH, Lu H, Cao GP. In situ synthesis of TS-1 on carbon nanotube decorated nickel foam with ultrafine nanoparticles and high content of skeleton titanium. Industrial and Engineering Chemistry Research. 2019;**58**:69-78. DOI: 10.1021/acs.iecr.8b04545

[6] Xiong G, Hu D, Guo Z, Meng Q, Liu L. An efficient titanium silicalite-1 catalyst for propylene epoxidation synthesized by a combination of aerosol-assisted hydrothermal synthesis and recrystallization. Microporous and Mesoporous Materials. 2018;**268**:93-99. DOI: 10.1016/j.micromeso.2018.04.015

[7] Li Y, Fan Q, Li Y, Feng X, Chai Y, Liu C. Seed-assisted synthesis of hierarchical nanosized TS-1 in a low-cost system for propylene epoxidation with H_2O_2. Applied Surface Science. 2019;**483**:652-660. DOI: 10.1016/j.apsusc.2019.03.334

[8] Wang B, Han H, Ge B, Ma J, Zhu J, Chen S. An efficient hydrophobic modification of TS-1 and its application in the epoxidation of propylene. New Journal of Chemistry. 2019;**43**:10390-10397. DOI: 10.1039/c9nj01937e

[9] Liu X, Liu J, Xia Y, Yin D, Steven RK, Mao L. Catalytic performance of TS-1 in oxidative cleavage of 1-alkenes with H_2O_2. Catalysis Communications. 2019;**126**:40-43. DOI: 10.1016/j.catcom.2019.04.021

[10] Martens JA, Buskens P, Jacobs PA, van der Pol A, van Hooff JHC, Ferrini C, et al. Hydroxylation of phenol with hydrogen peroxide on EUROTS-1 catalyst. Applied Catalysis A: General. 1993;**99**:71-84. DOI: 10.1016/0926-860X(93)85040-V

[11] Wu W, Tran DT, Wu X, Oh SC, Wang M, Chen H, et al. Multilamellar and pillared titanium silicalite-1 with long-range order of zeolite nanosheet layers: Synthesis and catalysis. Microporous and Mesoporous Materials. 2019;**278**:414-422. DOI: 10.1016/j.micromeso.2019.01.010

[12] Shen X, Wang J, Liu M, Li M, Lu J. Preparation of the hierarchical Ti-rich TS-1 via tritonX-100-assisted synthetic strategy for the direct oxidation of benzene. Catalysis Letters. 2019;**149**:2586-2596. DOI: 10.1007/s10562-019-02735-5

[13] Mantegazza MA, Leofanti G, Petrini G, Padovan M, Zecchina A, Bordiga S. Selective oxidation of ammonia to hydroxylamine with hydrogen peroxide on titanium based catalysts. Studies in Surface Science and Catalysis. 1994;**82**:541-550. DOI: 10.1016/S0167-2991(08)63447-3

[14] Hu Y, Dong C, Wang T, Luo G. Cyclohexanone ammoximation over TS-1 catalyst without organic solvent in a microreaction system. Chemical Engineering Science. 2018;**187**:60-66. DOI: 10.1016/j.ces.2018.04.044

[15] Xue Y, Zuo G, Wen Y, Wei H, Liu M, Wang X, et al. Seed-assisted synthesis of TS-1 crystals containing Al with high catalytic performances in cyclohexanone ammoximation. RSC Advances. 2019;**9**:2386-2394. DOI: 10.1039/c8ra10104c

[16] Huybrechts DRC, De Bruycker L, Jacobs PA. Oxyfunctionalization of alkanes with hydrogen peroxide on titanium silicalite. Nature. 1990;**345**:240-242. DOI: 10.1038/345240a0

[17] Zhu M, Zhu C, Wu D, Wang X, Wang H, Gao J, et al. Efficient photocatalytic water splitting through titanium silicalite stabilized CoO nanodots. Nanoscale. 2019;**11**:15984-15990. DOI: 10.1039/c9nr05057d

[18] Du Q, Guo Y, Wu P, Liu H, Chen Y. Facile synthesis of hierarchical TS-1 zeolite without using mesopore templates and its application in deep oxidative desulfurization. Microporous and Mesoporous Materials. 2019;**275**:61-68. DOI: 10.1016/j.micromeso.2018.08.018

[19] Chen R, Liu C, Johnson NW, Zhang L, Mahendra S, Liu Y, et al. Removal of 1,4-dioxane by titanium silicalite-1: Separation mechanisms and bioregeneration of sorption sites. Chemical Engineering Journal. 2019;**371**:193-202. DOI: 10.1016/j.cej.2019.03.285

[20] Millini R, Massara EP, Perego G, Bellussi G. Framework composition of titanium silicalite-1. Journal of Catalysis. 1992;**137**:497-503. DOI: 10.1016/0021-9517(92)90176-I

[21] Carati A, Flego C, Previde Massara E, Millini R, Carluccio L, Parker WO Jr, et al. Stability of Ti in MFI and Beta structures: A comparative study. Microporous and Mesoporous Materials. 1999;**30**:137-144. DOI: 10.1016/S1387-1811(99)00018-9

[22] Clerici MG, Ingallina P. Epoxidation of lower olefins with hydrogen peroxide and titanium silicalite. Journal of Catalysis. 1993;**140**:71-83. DOI: 10.1006/jcat.1993.1069

[23] Yoon CW, Hirsekorn KF, Neidig ML, Yang XZ, Tilley TD. Mechanism of the decomposition of aqueous hydrogen peroxide over heterogeneous TiSBA15 and TS-1 selective oxidation catalysts: Insights from spectroscopic and density functional theory studies. ACS Catalysis. 2011;**1**:1665-1678. DOI: 10.1021/cs2003774

[24] Guo Q, Sun K, Feng Z, Li G, Guo M, Fan F, et al. A thorough investigation of the active titanium species in TS-1 zeolite by in situ UV resonance Raman spectroscopy. Chemistry--A European Journal. 2012;**18**:13854-13860. DOI: 10.1002/chem.201201319

[25] Wang L, Xiong G, Su J, Li P, Guo H. In situ UV Raman spectroscopic study on the reaction intermediates for propylene epoxidation on TS-1. Journal of Physical Chemistry C. 2012;**116**:9122-9131. DOI: 10.1021/jp3017425

[26] Wang L, Wang X, Guo X, Li G, Xiu J. Quick synthesis of titanium silicalite-1. Chinese Journal of Catalysis. 2001;**22**:513-514. DOI: 0253-9837(2001)06-0513-02

[27] Zuo Y, Wang X, Guo X. Synthesis of titanium silicalite-1 with small crystal size by using mother liquid of titanium silicalite-1 as seed. Industrial and Engineering Chemistry Research. 2011;**50**:8485-8491. DOI: 10.1021/ie200281v

[28] Zuo Y, Liu M, Zhang T, Hong L, Guo X, Song C, et al. Role of pentahedrally coordinated titanium in titanium silicalite-1 in propene epoxidation. RSC Advances. 2015;**5**:17897-17904. DOI: 10.1039/c5ra00194c

[29] Fan WB, Duan RG, Yokoi T, Wu P, Kubota Y, Tatsumi T. Synthesis, crystallization mechanism, and catalytic properties of titanium-rich TS-1 free of extraframework titanium species. Journal of the American Chemical Society. 2008;**130**:10150-10164. DOI: 10.1021/ja7100399

[30] Wang J, Zhao YL, Yokoi T, Kondo JN, Tatsumi T. High-performance titanosilicate catalyst obtained through combination of liquid-phase and solid-phase transformation mechanisms. ChemCatChem. 2014;**6**:2719-2726. DOI: 10.1002/cctc.201402239

[31] Wang YM, He JQ. The method of adjusting pH value by oligosaccharide in the synthesis process of titanium silicalite. CN Patent. 2013;201210048648.7

[32] Zhang T, Zuo Y, Liu M, Song C, Guo X. Synthesis of titanium silicalite-1 with high catalytic performance for 1-butene epoxidation by eliminating the extraframework Ti. ACS Omega. 2016;**1**:1034-1040. DOI: 10.1021/acsomega.6b00266

[33] Zuo Y, Song W, Dai C, He Y, Wang M, Wang X, et al. Modification of small-crystal titanium silicalite-1 with organic bases: Recrystallization and catalytic properties in the hydroxylation of phenol. Applied Catalysis A: General. 2013;**453**:272-279. DOI: 10.1016/j.apcata.2012.12.027

[34] Zuo Y, Wang X, Guo X. Synthesis of titanium silicalite-1 with small crystal size by using mother liquor of titanium silicalite-1 as seeds (II): Influence of synthesis conditions on properties of titanium silicalite-1. Microporous and Mesoporous Materials. 2012;**162**:105-114. DOI: 10.1016/j.micromeso.2012.06.016

[35] Zuo Y, Liu M, Zhang T, Meng C, Guo X, Song C. Enhanced catalytic performance of titanium silicalite-1 in tuning the crystal size in the range 1200-200 nm in a tetrapropylammonium bromide system. ChemCatChem. 2015;**7**:2660-2668. DOI: 10.1002/cctc.201500440

[36] Wang Y, Zuo Y, Liu M, Dai C, Feng Z, Guo X. The high-performance hollow silicalite-1@titanium silicalite-1 core-shell catalyst for propene epoxidation. ChemistrySelect. 2017;**2**:10097-10100. DOI: 10.1002/slct.201701753

[37] Zuo Y, Liu M, Hong L, Wu M, Zhang T, Ma M, et al. Role of supports in the tetrapropylammonium hydroxide treated titanium silicalite-1 extrudates. Industrial and Engineering Chemistry Research. 2015;**54**:1513-1519. DOI: 10.1021/ie504531v

[38] Zuo Y, Liu M, Ma M, Wang Y, Guo X, Song C. Enhanced catalytic activity on post-synthesized hollow titanium silicalite-1 with high titanium content on the external surface. ChemistrySelect. 2016;**1**:6160-6166. DOI: 10.1002/slct.201601430

[39] Jacobsen CJH, Madsen C, Houzvicka J, Schmidt I, Carlsson A. Mesoporous zeolite single crystals. Journal of the American Chemical Society. 2000;**122**:7116-7117. DOI: 10.1021/ja000744c

[40] Zuo Y, Zhang T, Liu M, Ji Y, Song C, Guo X. Mesoporous/microporous titanium silicalite with controllable pore diameter for cyclohexene epoxidation. Industrial and Engineering Chemistry Research. 2018;**57**:512-520. DOI: 10.1021/acs.iecr.7b03719

[41] Zuo Y, Wang M, Song W, Wang X, Guo X. Characterization and catalytic performance of deactivated and regenerated TS-1 extrudates in a pilot plant of propene epoxidation. Industrial and Engineering Chemistry Research. 2012;**51**:10586-10594. DOI: 10.1021/ie300581z